RESEARCH ARTICLE

Chemical Characterisation of Organic Functional Group Compositions in $PM_{2.5}$ Collected at Nine Administrative Provinces in Northern Thailand during the Haze Episode in 2013

Siwatt Pongpiachan[1]*, Chomsri Choochuay[1], Jittiphan Chonchalar[1], Panatda Kanchai[1], Tidarat Phonpiboon[1], Sornsawan Wongsuesat[1], Kanokwan Chomkhae[2], Itthipon Kittikoon[2], Phoosak Hiranyatrakul[2], Junji Cao[3], Sombat Thamrongthanyawong[1]

Abstract

Along with rapid economic growth and enhanced agricultural productivity, particulate matter emissions in the northern cities of Thailand have been increasing for the past two decades. This trend is expected to continue in the coming decade. Emissions of particulate matter have brought about a series of public health concerns, particularly chronic respiratory diseases. It is well known that lung cancer incidence among northern Thai women is one of the highest in Asia (an annual age-adjusted incidence rate of 37.4 per 100,000). This fact has aroused serious concern among the public and the government and has drawn much attention and interest from the scientific community. To investigate the potential causes of this relatively high lung cancer incidence, this study employed Fourier transform infrared spectroscopy (FTIR) transmission spectroscopy to identify the chemical composition of the $PM_{2.5}$ collected using Quartz Fibre Filters (QFFs) coupled with MiniVol™ portable air samplers (Airmetrics). $PM_{2.5}$ samples collected in nine administrative provinces in northern Thailand before and after the "Haze Episode" in 2013 were categorised based on three-dimensional plots of a principal component analysis (PCA) with Varimax rotation. In addition, the incremental lifetime exposure to $PM_{2.5}$ of both genders was calculated, and the first derivative of the FTIR spectrum of individual samples is here discussed.

Keywords: $PM_{2.5}$ - FTIR - PCA - incremental lifetime exposure - northern provinces of Thailand

Asian Pacific J Cancer Prev, **14 (6)**, 3653-3661

Introduction

During the first two weeks of March 2013, agricultural waste burning, coupled with forest fires in northern regions of Thailand, steadily enhanced the levels of air pollution above the safety limit and produced an eye-stinging, throat-burning, yellow-tinged haze that reduced visibility to less than 1,000 metres. A profusion of fine particles, measuring less than 10 micrometres in diameter and known as PM_{10}, pervaded the atmosphere, reaching a peak on March 21st, 2013, at 428 $\mu g\ m^{-3}$ at Mae Hong Son province. This value was over 3.6 times the acceptable safety ceiling of 120 $\mu g\ m^{-3}$ and eventually prompted authorities to issue warnings against outdoor exercise. The monthly average concentrations of PM_{10} in March 2013 detected by the Pollution Control Department (PCD) of the Ministry of Natural Resources and Environment (MNRE) at Mae Hong Son (186±110 $\mu g\ m^{-3}$), Chiang Rai (122±71 $\mu g\ m^{-3}$), Lampang (123±75 $\mu g\ m^{-3}$), Phrae (123±58 $\mu g\ m^{-3}$) and Chiang Mai (124±11 $\mu g\ m^{-3}$) were slightly higher than the PCD 24-h standard. Several scientific studies have revealed that both long- and short-term exposure to $PM_{2.5}$ cause premature death and adverse cardiovascular effects, including enhanced hospitalisations and emergency department visits for heart attacks and strokes.

Atmospheric aerosol particles range in size over more than four orders of magnitude, from freshly nucleated clusters containing a few molecules to cloud droplets and crustal dust particles up to ten microns in size. Average particle compositions vary with size, time, and location, and the bulk compositions of individual particles of a given size also vary significantly. The size ranges of particles measured in urban centres are characterised according to three modes, with a minimum size between 1.0 μm and 3.0 μm. Particles with size ranges larger than the minimum size (super-micron particles) are referred to as "coarse",

[1]*NIDA Research Center of Disaster Prevention Management, School of Social and Environmental Development, National Institute of Development Administration (NIDA),* [2]*Bara Scientific Co., Ltd., Bangkok, Thailand,* [3]*SKLLQG, Institute of Earth Environment, Chinese Academy of Sciences (IEECAS), Xi'an, China *For correspondence: pongpiajun@gmail.com*

whereas smaller particles are called "fine". The three modes correspond to the nuclei mode (particles below 0.1 μm), accumulation mode (0.1<D_p<1 μm), and coarse mode (D_p>1 μm) (Whitby and Sverdrup, 1980). Thus, fine particles include both the accumulation and nuclei modes. Because the definition of modes has been based only on the mass (or volume distribution) of particles, the boundaries between these modes are not precise. The location of modes is dependent upon whether the modes are based on the particle number or surface distribution. In contrast, aerosols in rural areas are primarily of natural origin but are moderately influenced by anthropogenic sources (Hobbs et al., 1985). Recent studies have shown an association between $PM_{2.5}$ and adverse health effects, such as lung cancer (Pope et al., 2002) and heart attacks (Brook et al., 2002). Large particles (D_p>20 μm) deposit in the nasal passages, where they are removed by sneezing or swallowing. Finer particles, approximately 10 μm in diameter, can enter the respiratory system, and particles with diameters of less than 2.5 μm can penetrate even deeper into the lungs to the alveolar region, where they can remain for a long period of time (Harrison and Perry, 1986). In the urban atmosphere, polycyclic aromatic hydrocarbons (PAHs) are strongly associated with fine particles (Allen et al., 1996; Cecinato et al., 1999), although little data are available concerning the distribution of oxy PAHs within particulate matter (Allen et al., 1997). It is well known that PAHs are considered to pose potential health hazards because some PAHs are known carcinogens (Braga et al., 1999; Farmer et al., 2003). At ambient temperatures, two-ring naphthalene exists almost entirely in the gas phase, whereas five-ring PAHs and higher-ring PAHs are predominantly adsorbed onto particles. The intermediate three- and four-ring PAHs are distributed between the two phases (Zielinska et al., 2004).

Studies on the distribution of PAHs within the full size range of urban atmospheric particles found that 97% of the PAHs with five or more rings, which were all more or less completely particle-bound in the atmosphere, were associated with particles with aerodynamic diameters (d_{ac})<2.9 μm (Kauup et al., 2000). In the urban aerosols near the road measured in Guangzhou, China, approximately 57% of n-alkane and 62% of PAHs were found in the particle fraction with diameters<0.49 μm (Bi et al., 2004). The substance loading decreased steadily with increasing particle size. An average of only 1.2% of PAHs with five or more rings were found on large particles with d_{ac}>8.6 μm. In Pasadena, California, Miguel and Frielander (1978) reported that 72.7% and 76.8% of B[*a*]P and 75.7% and 93% of Cor sampled between October and December 1976, respectively, were present in particles with aerodynamic diameters in the range of 0.05-0.26 μm. In Hamilton, Ontario, the total particulate PAHs ranged between 87% and 95% and were found on particle sizes of 1.1 μm<*D*<7.0 μm (Katz and Chan, 1980). The relatively high proportion of particulate PAHs (63% to 85%) measured in London were found in aerosols with aerodynamic diameters of less than 1.1 μm, and up to 95% of particulate PAHs in London were associated with particles under 3.3 μm in diameter (Baek et al., 1991).

Unlike in other developed countries, there are a limited number of studies concerning the chemical characterisation of gaseous species and aerosols in Thailand (Thumanu et al., 2009; Pongpiachan, 2013a; 2013b; Pongpiachan et al., 2010, 2012a; 2012b; 2012c, 2013a; 2013b). In this study, the authors postulate that the use of Fourier Transform Infrared Spectroscopy (FTIR), combined with numerous analogies of statistical analysis, assist in a better understanding of the distribution pattern of organic functional compositions of $PM_{2.5}$, which can be subjected to variations in sources and meteorological conditions in northern Thailand. It is the objective of this study to demonstrate the general application of organic functional group analysis by FTIR as an innovative indicator to chemically characterise $PM_{2.5}$ at nine provinces in the northern region of Thailand "before" and "after" the haze episode in 2013. In addition, the incremental lifetime exposure to $PM_{2.5}$ and the application of FTIR spectral features as an alternative "*Biomass Burning*" proxy will be reviewed and discussed.

Materials and Methods

Monitoring sites and sampling period

Monitoring of $PM_{2.5}$ was conducted at nine locations and over several time periods. In all instances, the duration of each sample collection was 24 h. The sampling campaigns can be grouped according to the observation period during which they were conducted: *campaign I* was carried out before the "haze episode" in the winter of 2012 (i.e., from the 7th to 22nd of December 2012), whereas monitoring during *campaign Π* was conducted in March 2013 (i.e., from the 4th to 19th of March 2013; see Table 1). Both monitoring campaigns were performed at nine observatory sites, namely, Chiang-Rai Province Observatory Site (CROS; The Eight Hotel; E: 593783, N: 2258302); Chiang-Mai Province Observatory Site (CMOS; Yupparat School; E: 498805, N: 2077713); Nan Province Observatory Site (NPOS; Thewarat Hotel; E: 687123, N: 2077209); Phayao Province Observatory Site (PYOS; Arunothai Coffee House Homestay; E: 594420, N: 2119215); Mae Hong Son Province Observatory Site (MHOS; Mae Hong Son Provincial Forestry Office; E: 391834, N: 2134869); Phrae Province Observatory Site (PHOS; Nana Charoenmuang Hotel; E: 620935, N: 2006155); Lampang Province Observatory Site (LMOS; Maemoh Training Center; E: 568200, N: 2020017); Lamphun Province Observatory Site (LPOS; Lamphun Provincial Administration Organization Stadium; E: 500441, N: 2052987); and Uttaradit Province Observatory Site (UTOS; OUM Hotel; E: 615923, N: 1948269) (Figure 1). There were no obstructions in the vicinity of the sampling equipment, which was strategically positioned to be accessible to winds from all directions. Monitoring at group-1 monitoring stations (CROS, PYOS and NPOS), group-2 monitoring stations (LMOS, PHOS and UTOS) and group-3 monitoring stations (MHOS, CMOS and LPOS) was conducted synchronously every day from the 28th of November to the 4th of December 2012, from the 7th to 13th of December 2012 and from the 16th to 22nd of December 2012, respectively, as summarised in Table 1.

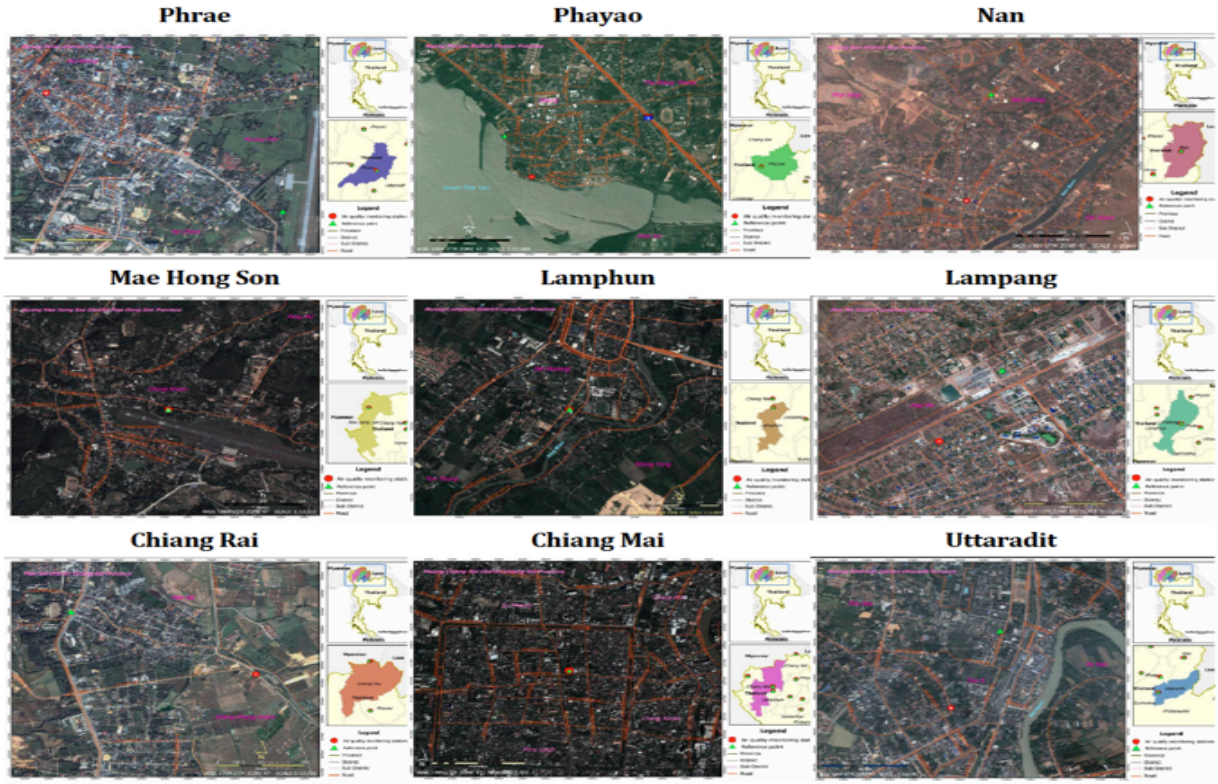

Figure 1. Maps of Air Quality Observatory Sites at Nine Provinces of Upper Part of Northern Thailand

Sampling equipment

MiniVol™ portable air samplers (Airmetrics) were used to collect $PM_{2.5}$ over a 24 h period at nine sampling sites. The MiniVol's pump draws air at 5 litres $minute^{-1}$ through a particle size separator (impactor) and then through a 47 mm filter. A 2.5 micron particle separation is achieved by impaction. Neither PM_{10} nor TSP samples were collected for this study.

FTIR analysis

It is well known that Fourier Transform Infrared (FTIR) spectrophotometry provides at least three major advantages. These advantages include a multiplex advantage (i.e., the accumulation of the results is accomplished by measuring a spectrum of all wavenumbers with relatively high scanning speed); an aperture advantage (i.e., the sensitivity of FTIR results depends on the aperture area and the incident angle of light); and a wavenumber accuracy advantage (i.e., the laser emits extremely stable monochromatic light, generating a spectrum with high wavenumber accuracy). In this study, IR-Affinity-1 Shimadzu was chosen because it possesses the following traits: (i) high measurement sensitivity, (ii) measurement of samples with low transmittance, (iii) higher speed measurement, (iv) higher wavenumber accuracy and (v) highly accurate spectrum subtraction.

The process of FTIR transmission spectroscopy involves detecting the absorption of an infrared beam that is passed directly through the sample and through Quartz Fibre Filters (QFFs). Because the resulting absorption bands are unique to specific functional groups and because these bands are proportional to the amount of sample present, a functional group analysis can be performed using FTIR to provide quantitative and qualitative information. Subtraction of the blank (i.e., the spectrum of the empty QFFs) from the filtered sample was performed for each sample. Each spectrum was determined by averaging 16 scans at a resolution of 2 cm^{-1}. The spectra describe the absorbance of radiation as a function of wavenumber, which ranges from 4,000-400 cm^{-1}. For more details on the quantification of identified functional groups in $PM_{2.5}$ samples collected on QFFs, please refer to a previous publication by Krost and McClenney (1994).

Statistical analysis

SPSS version 13 was used to calculate the average values, standard deviations and principal component analysis with Varimax rotation of the data set.

Results and Discussion

$PM_{2.5}$ concentrations

All $PM_{2.5}$ samples were identified successfully in both sampling campaigns (n=126). Table 1 summarises the average concentrations of $PM_{2.5}$ measured in the seven samples taken before and after the "Haze Episode" at CROS, PYOS, NPOS, LMOS, PHOS, UTOS, MHOS, CMOS and LPOS. The atmospheric concentrations of individual $PM_{2.5\text{-before the "Haze Episode"}}$ collected from nine observatory sites varied from 1.38 to 100.69 μg m^{-3}, with an average of 35.16±19.59 μg m^{-3}, whereas the $PM_{2.5\text{-after the "Haze Episode"}}$ samples ranged from 20.69 to 517.24 μg m^{-3}, with an average of 96.14±47.27 μg m^{-3}. The seven-day $PM_{2.5}$ average was found to be the highest at MHOS after the "Haze Episode," with an atmospheric concentration of 209.85±91.67 μg m^{-3}, whereas the lowest concentration was observed at CROS, with an average value of 14.98±6.09 μg m^{-3}. It is interesting to note that the $PM_{2.5}$-

Table 1. $PM_{2.5}$ Concentrations Before and After the "2013 Haze Episode" at Nine Provinces of Northern Part of Thailand

Sampling Site	$PM_{2.5}$ before the "haze episode"		$PM_{2.5}$ after the "haze episode"		Change in $PM_{2.5}$ Mass Concentration		
	Sampling Date	$PM_{2.5}$ ($\mu g\ m^{-3}$)	Sampling Date	$PM_{2.5}$ ($\mu g\ m^{-3}$)	$PM_{2.5}$ after-$PM_{2.5}$ before ($\mu g\ m^{-3}$)		Percentage Change (%)
CROS	11/28/12	12.41	2/23/56	85.52	73.10	Increase	589
	11/29/12	15.17	2/24/56	59.31	44.14	Increase	291
	11/30/12	24.83	2/25/56	74.48	49.66	Increase	200
	12/1/12	8.28	2/26/56	84.14	75.86	Increase	917
	12/2/12	20.69	2/27/56	99.31	78.62	Increase	380
	12/3/12	13.79	2/28/56	102.07	88.28	Increase	640
	12/4/12	9.66	3/1/56	137.93	128.28	Increase	1,329
	Average	**14.98±6.09**		**91.82±30.90**	**76.85±30.47**	**Increase**	**513±350**
PYOS	11/28/12	15.17	2/23/56	62.07	46.90	Increase	309
	11/29/12	9.66	2/24/56	62.07	52.41	Increase	543
	11/30/12	22.07	2/25/56	93.79	71.72	Increase	325
	12/1/12	16.55	2/26/56	97.93	81.38	Increase	492
	12/2/12	8.28	2/27/56	99.31	91.03	Increase	1,100
	12/3/12	17.93	2/28/56	140.69	122.76	Increase	685
	12/4/12	34.48	3/1/56	142.07	107.59	Increase	312
	Average	**17.73±9.30**		**99.70±41.37**	**81.97±34.81**	**Increase**	**462±305**
NPOS	11/28/12	24.83	2/23/56	46.90	22.07	Increase	89
	11/29/12	20.69	2/24/56	59.31	38.62	Increase	187
	11/30/12	17.93	2/25/56	52.41	34.48	Increase	192
	12/1/12	27.59	2/26/56	64.83	37.24	Increase	135
	12/2/12	13.79	2/27/56	102.07	88.28	Increase	640
	12/3/12	26.21	2/28/56	107.59	81.38	Increase	311
	12/4/12	35.86	3/1/56	106.21	70.34	Increase	196
	Average	**23.84±9.66**		**77.04±36.95**	**53.20±31.03**	**Increase**	**223±174**
LMOS	12/7/12	12.41	3/4/56	57.93	45.52	Increase	367
	12/8/12	33.10	3/5/56	55.17	22.07	Increase	67
	12/9/12	35.86	3/5/56	64.83	28.97	Increase	81
	12/10/12	26.21	3/6/56	84.14	57.93	Increase	221
	12/11/12	33.10	3/7/56	66.21	33.10	Increase	100
	12/12/12	23.45	3/8/56	75.86	52.41	Increase	224
	12/13/12	38.62	3/9/56	146.21	107.59	Increase	279
	Average	**28.97±11.37**		**78.62±34.16**	**49.66±28.09**	**Increase**	**171±116**
PHOS	12/7/12	52.41	3/4/56	30.34	-22.07	Decrease	42
	12/8/12	64.83	3/5/56	53.79	-11.03	Decrease	17
	12/9/12	71.72	3/5/56	67.59	-4.14	Decrease	6
	12/10/12	100.69	3/6/56	49.66	-51.03	Decrease	51
	12/11/12	78.62	3/7/56	517.24	438.62	Increase	558
	12/12/12	66.21	3/8/56	91.03	24.83	Increase	38
	12/13/12	56.55	3/9/56	120.00	63.45	Increase	112
	Average	**70.15±28.69**		**132.81±155.33**	**62.66±148.37**	**Increase**	**89±222**
UTOS	12/7/12	49.66	3/4/56	20.69	-28.97	Decrease	58
	12/8/12	46.90	3/5/56	23.45	-23.45	Decrease	50
	12/9/12	73.10	3/5/56	75.86	2.76	Increase	4
	12/10/12	64.83	3/6/56	68.97	4.14	Increase	6
	12/11/12	68.97	3/7/56	67.59	-1.38	Decrease	2
	12/12/12	17.93	3/8/56	88.28	70.34	Increase	392
	12/13/12	28.97	3/9/56	78.62	49.66	Increase	171
	Average	**50.05±24.58**		**60.49±31.99**	**10.44±33.24**	**Increase**	**21±132**
MHOS	12/16/12	64.83	3/13/56	171.03	106.21	Increase	164
	12/17/12	22.07	3/14/56	212.41	190.34	Increase	862
	12/18/12	33.10	3/15/56	204.14	171.03	Increase	517
	12/19/12	38.62	3/16/56	204.14	165.52	Increase	429
	12/20/12	23.45	3/17/56	184.83	161.38	Increase	688
	12/21/12	33.10	3/18/56	182.07	148.97	Increase	450
	12/22/12	26.21	3/19/56	310.34	284.14	Increase	1,084
	Average	**34.48±17.50**		**209.85±91.67**	**175.37±85.26**	**Increase**	**509±619**
CMOS	12/16/12	20.69	3/13/56	60.69	40.00	Increase	193
	12/17/12	38.62	3/14/56	53.79	15.17	Increase	39
	12/18/12	22.07	3/15/56	52.41	30.34	Increase	137
	12/19/12	52.41	3/16/56	48.28	-4.14	Decrease	8
	12/20/12	53.79	3/17/56	57.93	4.14	Increase	8
	12/21/12	27.59	3/18/56	88.28	60.69	Increase	220
	12/22/12	46.90	3/19/56	131.03	84.14	Increase	179
	Average	**37.44±16.78**		**70.34±35.96**	**32.91±31.05**	**Increase**	**88±85**

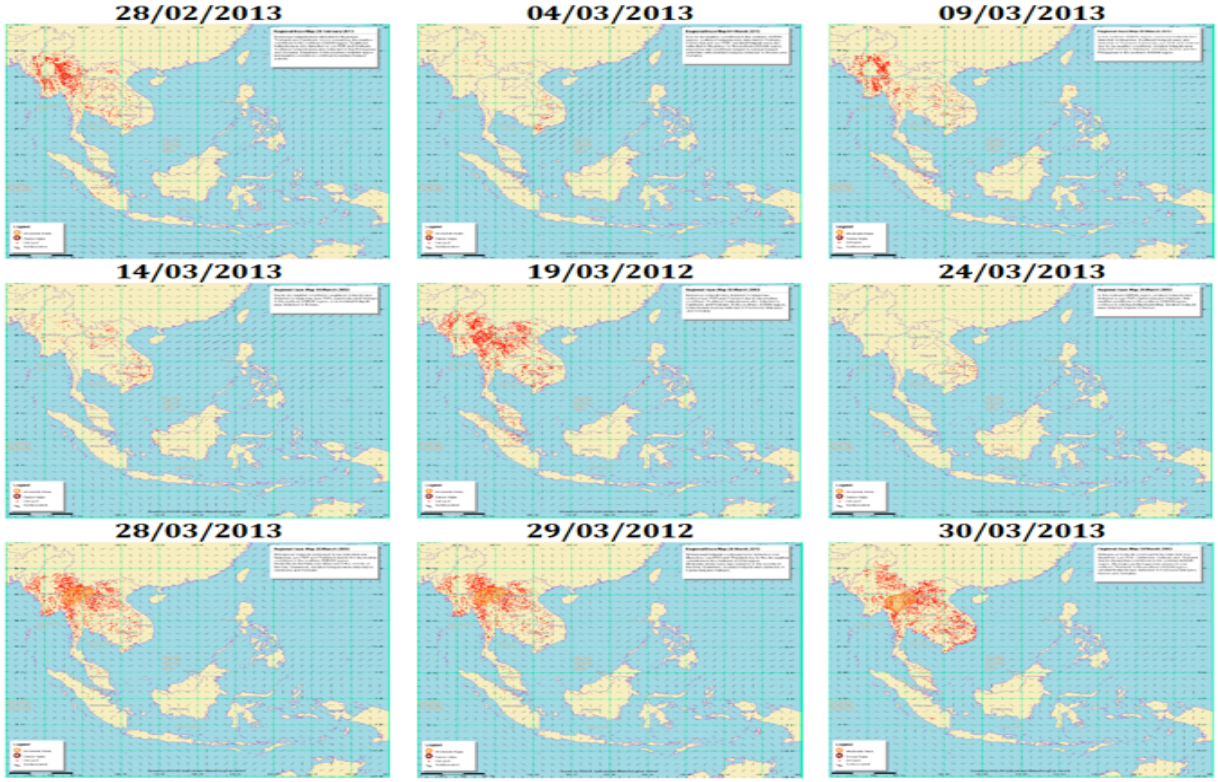

Figure 2. Spatial and Temporal Distribution of Wind Directions and Hot Spots in Thailand from 28th February to 30th March 2013 (ASEAN Regional Specialized Meteorological Centre, Singapore)

$_{\text{before the "Haze Episode"}}$ concentrations, in decreasing order, are PHOS (70.15±28.69 μg m^{-3})>UTOS (50.05±24.58 μg m^{-3})>LPOS (38.82±17.81 μg m^{-3})>CMOS (37.44±16.78 μg m^{-3})>MHOS (34.48±17.50 μg m^{-3})>LMOS (28.97±11.37 μg m^{-3})>NPOS (23.84±9.66 μg m^{-3})>PYOS (17.73±9.30 μg m^{-3})>CROS (14.98±6.09 μg m^{-3}), whereas those after the "Haze Episode" are MHOS (209.85±91.67 μg m^{-3})>LPOS (140.69±62.27 μg m^{-3})>PHOS (132.81±155.33 μg m^{-3})>PYOS (99.70±41.37 μg m^{-3})>CROS (91.82±30.90 μg m^{-3})>LMOS (78.62±34.16 μg m^{-3})>NPOS (77.04±36.95 μg m^{-3})>CMOS (70.34±35.96 μg m^{-3})>UTOS (60.49±31.99 μg m^{-3}) (see Table 1). It is also worth mentioning that the percentage increases of $PM_{2.5}$, in descending order, are CROS (513±350%)>MHOS (509±619%)>PYOS (462±305%)>LPOS (262±277%)>NPOS (223±174%)>LMOS (171±116%)>PHOS (89±222%)>CMOS (88±85%)>UTOS (21±132%).

Characteristics of FTIR spectra and their first derivatives

As illustrated in Figure 3 and Figure 4, $PM_{2.5\text{-before the "Haze Episode"}}$ has more complicated FTIR spectra coupled with their first derivatives than those of $PM_{2.5\text{-after the "Haze Episode"}}$. The main IR absorption band of $PM_{2.5\text{-before the "Haze Episode"}}$ in samples collected at PYOS, CMOS, NPOS and MHOS appears at approximately 405 cm^{-1}, 430 cm^{-1}, 463 cm^{-1} and 496 cm^{-1}, respectively. These FTIR spectra characteristics reflect more complicated chemical mixtures released from the unique emission sources of each province before the "Haze Episode". In normal conditions, both "anthropogenic activities" and "natural emissions" appear to play an important role in governing the organic functional group content of $PM_{2.5}$. In contrast, the major IR absorption band of $PM_{2.5\text{-after the "Haze Episode"}}$ in samples collected at MHOS, PYOS, PHOS and CROS occurs at approximately 405 cm^{-1}, 409 cm^{-1}, 409 cm^{-1} and 486 cm^{-1}, respectively. These results indicate that $PM_{2.5\text{-after the "Haze Episode"}}$ is comparatively more homogeneous than $PM_{2.5\text{-before the "Haze Episode"}}$. This homogeneity was possibly caused by the overwhelming amount of biomass-burning aerosols present in the nine administrative northern provinces after the "Haze Episode".

Occupational exposure of outdoor workers to $PM_{2.5}$

To assess the health risks associated with the occupational exposure of outdoor workers to $PM_{2.5}$, the incremental lifetime particulate matter exposure (***ILPE***) model was employed and defined as follows:

$$ILPE = C \times IR \times t \times EF \times ED \qquad \textbf{Equation 1}$$

ILPE=Incremental lifetime particulate matter exposure (g), ***C***=$PM_{2.5}$ concentrations (μg m^{-3}), ***IR***=Inhalation rate (m^3 h^{-1}), *t*=Daily exposure time span (6 h d^{-1}, for two shifts), ***EF***=Exposure frequency (250 d $year^{-1}$ [a], upper-bound value), and ***ED***=Exposure duration (25 years[a], upper-bound value). Note: [a]Adapted from Human Health Evaluation Manual (US EPA, 1991).

According to the methods for the derivation of inhalation dosimetry (US EPA, 1994), the inhalation rates of male and female outdoor workers were estimated to be 0.89 and 0.49 m^3 h^{-1}, respectively. The ***ILPE*** model was adapted from the probabilistic incremental lifetime cancer risk (*ILCR*) model, which was used to assess traffic policemen's exposure to PAHs during their work in China (Hu et al., 2007). The estimated ***ILPE*** levels in outdoor workers are summarised in Table 2. The predicted ***ILPE*** of $PM_{2.5}$ was consistently highest in both genders at MHOS after the "Haze Episode", with average values of 7,004±3,059 mg and 3,856±1,684 mg for $PM_{2.5}$

accumulated in male and female workers, respectively, over an exposure duration of 25 years. These increased concentrations of $PM_{2.5}$ after the "Haze Episode" may have several explanations, including not only vehicular and other industrial emissions but also agricultural waste burning in suburban regions. It is well known that uncontrolled biomass burning and forest fires have been found to be significant sources of ambient $PM_{2.5}$ in Mae Hong Son and other northern cities over recent decades, particularly during cold periods. An inversion is more likely to arise during the winter when the angle of the sun is very low, predominantly in mountainous provinces such as Mae Hong Son, and could theoretically be accountable for the rise of $PM_{2.5}$ content during the observation periods from the 13th to 19th of March 2013. The relatively low ***ILPE*** of $PM_{2.5}$ observed at CMOS (i.e., 2,348±1,200 mg and 1,292±661 mg for males and females, respectively) highlights the effects of anti-burning and smog prevention programs proactively enacted by local administration organisations since November 2011. It is also interesting to note that the ***ILPE*** of $PM_{2.5}$ at CROS after the "Haze Episode" (i.e., 3,064±1,031 mg and 1,687±568 mg for males and females, respectively) is approximately six times higher than that during normal conditions (i.e., 500±203 mg and 275±112 mg for males and females, respectively). This difference in the ***ILPE*** of $PM_{2.5}$ at CROS can be explained by the occurrence of comparatively more hot spots during the monitoring period after the "Haze Episode" (Figure 2).

Table 2. Statistical Description of the Inhaled Particulate Mass of $PM_{2.5}$ at Nine Administrative Provinces in Northern Part of Thailand*

	Before the "Haze Episode"		After the "Haze Episode"	
	$PM_{2.5}$ (mg) Male	$PM_{2.5}$ (mg) Female	$PM_{2.5}$ (mg) Male	$PM_{2.5}$ (mg) Female
CROS	500±203	275±112	3,064±1,031	1,687±568
LMOS	967±379	532±209	2,624±1,140	1,445±628
LPOS	1,296±594	713±327	4,696±2,078	2,585±1,144
CMOS	1,250±560	688±308	2,348±1,200	1,292±661
MHOS	1,151±584	634±322	7,004±3,059	3,856±1,684
PYOS	592±310	326±171	3,327±1,381	1,832±760
NPOS	796±322	438±178	2,571±1,233	1,416±679
PHOS	2,341±958	1,289±527	4,433±5,184	2,440±2,854
UTOS	1,670±820	920±452	2,019±1,068	1,112±588

*Inhaled particulate mass over exposure duration of 25 years. **Values represent average±standard deviation

Pearson correlation analysis

Pearson correlation coefficients of averaged FTIR spectra of $PM_{2.5}$ collected before and after the "Haze Episode" are displayed in Table 3. Only three combinations, namely CROS-LMOS (R=0.83), CROS-LPOS (R=0.88) and LMOS-LPOS (R=0.71), have R-values higher than 0.7 before major biomass burning events (Table 3). Interestingly, relatively high correlations between FTIR spectra of CROS-LMOS (R=0.98), CROS-LPOS (R=0.95), CROS-CMOS (R=0.76), CROS-NPOS (R=0.95), LMOS-LPOS (R=0.97), LMOS-CMOS (R=0.72), LMOS-NPOS (R=0.98), LPOS-CMOS (R=0.72), LPOS-NPOS (R=0.99), CMOS-NPOS (R=0.71) and PYOS-PHOS (R=0.99) were observed after the forest fire events. As previously mentioned, these findings are consistent with the FTIR spectra results together with their corresponding first derivatives, emphasising the strong dominance of biomass burning over the chemical characteristics of organic functional groups in $PM_{2.5}$ (Figure 3 and Figure 4). It is worth mentioning that the R-values higher than 0.7 are combinations of administrative provinces that share the same border lines and/or vegetation types. In contrast, relatively low R-values (less than 0.3) were observed at administrative provinces that have strong dissimilarities in both geographical conditions and forest types, such as CMOS-MHOS (R=0.20), MHOS-PYOS (R=0.25), MHOS-PHOS (R=0.25) and MHOS-UTOS (R=0.22) (see Table 3).

Principal component analysis

PCA is employed as a multivariate analytical tool

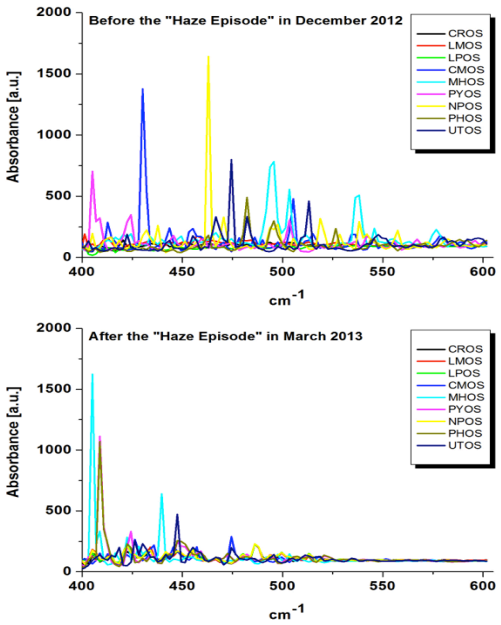

Figure 3. FTIR Spectrum of $PM_{2.5}$ from Wave Number 400 to 600 cm^{-1}

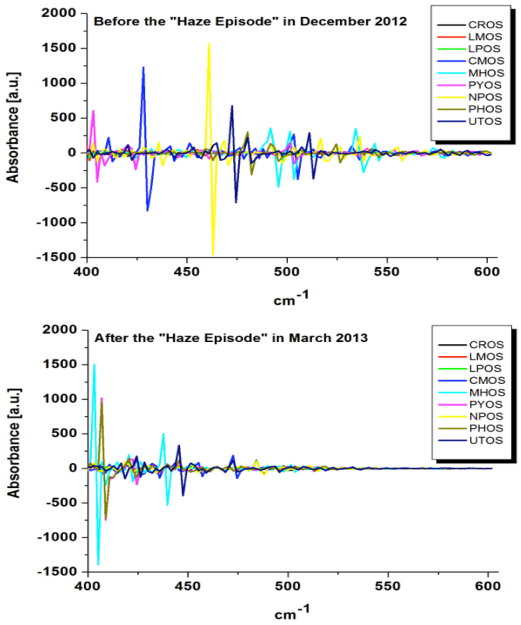

Figure 4. First Derivative of FTIR Spectrum of $PM_{2.5}$ from Wave Number 400 to 600 cm^{-1}

Table 3. Pearson Correlation Coefficients of Averaged FTIR Spectrum of $PM_{2.5}$ Collected during Periods of "before" and "after" the Haze Episode

	*B-CROS	B-LMOS	B-LPOS	B-CMOS	B-MHOS	B-PYOS	B-NPOS	B-PHOS	B-UTOS	A-CROS	A-LMOS	A-LPOS	A-CMOS	A-MHOS	A-PYOS	A-NPOS	A-PHOS	A-UTOS
B-CROS	1.000																	
B-LMOS	**0.831**	1.000																
B-LPOS	**0.876**	**0.705**	1.000															
B-CMOS	0.014	0.105	-0.093	1.000														
B-MHOS	0.086	0.116	-0.091	0.200	1.000													
B-PYOS	-0.046	0.046	-0.182	0.240	0.308	1.000												
B-NPOS	0.031	0.111	-0.059	0.239	0.282	0.218	1.000											
B-PHOS	0.030	0.052	0.048	0.222	0.396	0.309	0.362	1.000										
B-UTOS	0.031	0.094	-0.033	0.162	0.198	0.296	0.172	0.466	1.000									
**A-CROS	**0.817**	**0.830**	0.663	0.091	0.109	0.097	0.017	0.008	-0.004	1.000								
A-LMOS	**0.764**	**0.790**	0.580	0.134	0.154	0.210	0.031	0.017	0.013	**0.975**	1.000							
A-LPOS	**0.742**	**0.794**	0.523	0.160	0.209	0.209	0.055	0.028	0.063	**0.948**	**0.973**	1.000						
A-CMOS	**0.758**	**0.791**	0.609	0.032	0.037	0.043	0.005	-0.052	0.195	**0.760**	**0.724**	**0.717**	1.000					
A-MHOS	0.189	0.281	0.054	0.013	0.028	0.605	0.055	-0.053	-0.021	0.311	0.406	0.362	0.202	1.000				
A-PYOS	0.373	0.440	0.236	0.028	0.056	0.286	-0.001	-0.072	0.011	0.390	0.422	0.404	0.451	0.246	1.000			
A-NPOS	**0.736**	**0.774**	0.509	0.145	0.209	0.246	0.049	0.032	0.056	**0.953**	**0.978**	**0.986**	**0.710**	0.397	0.428	1.000		
A-PHOS	0.388	0.448	0.248	0.033	0.049	0.267	-0.001	-0.084	0.004	0.399	0.429	0.406	0.455	0.251	**0.991**	0.437	1.000	
A-UTOS	0.650	0.662	0.503	0.233	0.090	0.037	0.014	-0.039	0.099	0.692	0.653	0.650	0.741	0.218	0.393	0.643	0.403	1.000

*B: Before, **A: After

Figure 5. Three-Dimensional Plots of PC1, PC2 and PC3 Using FTIR Spectrum from Wave Number 400 to 4000 cm^{-1}

to reduce a set of original variables (measured FTIR spectra in $PM_{2.5}$ samples) and to extract a small number of latent factors (principal components, PCs) to analyse relationships among the observed variables. Data submitted for this analysis were arranged in a matrix, where each column corresponds to one FTIR spectrum and each row represents the number of samples. Data matrixes were evaluated through PCA, allowing the summarised data to be further analysed and plotted. To enable further interpretation of potential sources of organic functional groups in $PM_{2.5}$, a PCA model with three significant principal components (PCs) was calculated. Each PC of this model represented 43.06%, 13.67% and 9.85% of the variance, thus accounting for 66.58% of the total variation in the data.

These correlation coefficients of each PC are quite useful and provide valuable information that can be used to identify biomass-burning aerosols. However, these correlation coefficients, as well as source profiles, should be used with great caution because physiochemical processes can alter chemical composition distribution patterns during transport from the emission source to the receptor site. To minimise the above-mentioned uncertainties, the plots of three-dimensional PCs can be used as a tool to characterise aerosol types during the sampling period. The clearest features displayed in Figure 5 are described as follows: (i) 3D plots of B-CMOS, B-MHOS, B-PYOS, B-NPOS and B-PHOS, suggesting that the majority of $PM_{2.5}$ before the "Haze Episode" had similar organic functional compositions; (ii) 3D plots of groups of $PM_{2.5}$ after the "Haze Episode" are highly clustered, indicating that the majority of $PM_{2.5}$ shared comparable chemical compositions during the biomass-burning events; (iii) there are distinctly different sources of $PM_{2.5}$ before and after the "Haze Episode", indicating that FTIR spectra, coupled with PCA, can successfully distinguish "*background aerosols*" from "*biomass-burning aerosols*"; and (iv) the 3D plot of the B-LPOS strongly deviates from the group in both sampling campaigns, implying that other unique local emission

sources might be significant in Lamphun province.

In conclusions, FTIR spectra of $PM_{2.5}$ collected before and after the "Haze Episode" at nine administrative provinces in northern Thailand were analysed by IR-Affinity-1 Shimadzu. In general, $PM_{2.5\text{-before the "Haze Episode"}}$ samples have more complicated FTIR spectra than those of background aerosols, emphasising that "*Biomass Burning*" played an important role in governing aerosol chemical compositions in March 2013. The predicted ***ILPE*** of $PM_{2.5}$ indicated maximum values at MHOS in both genders after the "*Haze Episode*", with average values of 7,004±3,059 mg and 3,856±1,684 mg for $PM_{2.5}$ accumulated in male and female workers, respectively, over an exposure duration of 25 years. The relatively low ***ILPE*** of $PM_{2.5}$ observed at CMOS (i.e., 2,348±1,200 mg and 1,292±661 mg for males and females, respectively) highlights the effects of anti-burning and smog prevention programs proactively enacted by local administration organisations since November 2011. In conclusion, 3D plots of PCA, coupled with FTIR spectra, successfully discriminated "*Biomass-Burning Aerosols*" from "*Background Aerosols*", suggesting that FTIR analysis can be used as an alternative tool to characterise types of aerosols.

Acknowledgements

This project was financed by National Institute of Development Administration (NIDA) Research Center. The author acknowledges Assist. Prof. Dr. Torpong Kreetachart from School of Energy and Environment (SEEN), University of Phayao for their contributions on laboratory works. The authors thank the kind support from Pollution Control Department, Ministry of Natural Resources and Environment for providing meteorological data.

References

Allen JO, Dookeran NM, Smith KA, et al (1996). Measurement of polycyclic aromatic hydrocarbons associated with size-segregated atmospheric aerosols in Massachusetts. *Environ Sci Technol*, **30**, 1023-31.

Allen JO, Dookeran NM, Smith KA, et al (1997). Measurement of oxygenated polycyclic aromatic hydrocarbons associated with size-segregated urban aerosol. *Environ Sci Technol*, **31**, 2064-70.

Baek SO, Goldstone ME, Kirk PW (1991). Phase distribution and particle size dependency of polycyclic aromatic hydrocarbons in the urban atmosphere. *Chemosphere*, **22**, 503-20.

Bi X, Peng P, Chen Y, Fu C (2004). Size distribution of n-alkanes and polycyclic aromatic hydrocarbons in urban and rural atmospheres of Guangzhou, China. *Atmos Environ*, **39**, 477-87.

Braga RS, Barone PMVB, Galvão DS (1999). Identifying carcinogenic activity of methylated polycyclic aromatic hydrocarbons (PAHs). *J Mol Struct*, **464**, 257-66.

Brook DR, Brook RJ, Urch B, et al (2002). Inhalation of fine particulate air pollution and ozone causes acute arterial vasoconstriction in healthy adults. *Circulation*, **105**, 1534-6.

Cecinato A, Marino F, Filippo P, Lepore L, Possanzini M (1999). Distribution of n-alkanes, polynuclear aromatic hydrocarbons and nitrated aromatic hydrocarbons between the fine and coarse fractions of inhalable atmospheric particulates. *J Chromatogr A*, **846**, 255-64.

Farmer PB, Singh R, Kaur B, et al (2003). Molecular epidemiology studies of carcinogenic environmental pollutants: effects of polycyclic aromatic hydrocarbons (PAHs) in environmental pollution on exogenous and oxidative DNA damage. *Mutat Res-Rev Mutat*, **544**, 397-402.

Harrison RM, Perry R (Editors) (1986) Handbook of air pollution analysis, Chapman and Hall, London.

Hobbs PV, Bowdle DA, Radke LF (1985). Particles in the lower troposphere over the high plains of the United States. 1. Size distributions, elemental compositions, and morphologies. *J Climate Appl Meteorol*, **24**, 1344-56.

Hu Y, Bai Z, Zhang L, et al (2007). Health risk assessment for traffic policemen exposed to polycyclic aromatic hydrocarbons (PAHs) in Tianjin, China. *Sci Tot Environ*, **382**, 240-50.

Katz M, Chan C (1980). Comparative distributions of eight polycyclic aromatic hydrocarbons in airborne particulates collected by conventional high-volume sampling and by size fractionation. *Environ Sci Technol*, **14**, 838-43.

Kaupp H, McLachlan MS (2000). Distribution of polychlorinated dibenzo-p-dioxins and dibenzofurans (PCDD/Fs) and polycyclic aromatic hydrocarbons (PAHs) within the full size range of atmospheric particles. *Atmos Environ*, **34**, 73-83.

Krost KJ, McClenney WA (1994). FT-IT transmissions spectroscopy for quantification of ammonium bisulfate in fine-particulate matter collected on Teflon® filters. *Appl Spectrosc*, **48**, 702-5.

Miguel AH, Friedlander SK (1978). Distribution of benzo[*a*] pyrene and coronene with respect to particle size in Pasadena aerosols in the submicron range. *Atmos Environ*, **12**, 2407-13.

Pongpiachan S, Surapipit V, Ketratanakul A, Wuttijak N, Pongnoppa A (2010). Risk analysis by emission source strengths and wind directions of trace gases at Map Ta Phut Industrial Estate, Rayong province, Thailand. Risk Analysis VII, WIT press, pp. 337-47.

Pongpiachan S, Surapipit V, Hirunyatrakul P, et al (2012). Application of Air Compass Model for Source Identification of Trace Gaseous from Seven Air Quality Monitoring Stations of Pollution Control Department in Bangkok, Thailand. Air Pollution XX, WIT press, pp. 179-88.

Pongpiachan S, Thumanu K, Na Pattalung W, et al (2012). Diurnal variation and spatial distribution effects of sulfur speciation in aerosol samples as assessed by X-ray Absorption Near-edge Structure (XANES). *J Anal Methods Chem*, **2012**, 696080.

Pongpiachan S, Thumanu K, Kositanont C, et al (2012). Parameters influencing sulfur speciation in environmental samples using sulfur K-Edge X-Ray Absorption Near-Edge Structure (XANES). *J Anal Methods Chem*, **2012**, 659858.

Pongpiachan S, Choochuay C, Hattayanone M, Kositanont C (2013). Temporal and spatial distribution of particulate carcinogens and mutagens in Bangkok, Thailand. *Asian Pac J Cancer Prev*, **14**, 1879-87.

Pongpiachan S (2013). Vertical distribution and potential risk of particulate polycyclic aromatic hydrocarbons in high buildings of Bangkok, Thailand. *Asian Pac J Cancer Prev*, **14**, 1865-77.

Pongpiachan S (2013). Diurnal variation, vertical distribution and source apportionment of carcinogenic Polycyclic Aromatic Hydrocarbons (PAHs) in Chiang-Mai, Thailand. *Asian Pac J Cancer Prev*, **14**, 1851-63.

Pongpiachan S, Ho KF, Cao J (2013). Estimation of gas-particle partitioning coefficients (Kp) of carcinogenic polycyclic

aromatic hydrocarbons by carbonaceous aerosols collected at Chiang-Mai, Bangkok and Hat-Yai, Thailand. *Asian Pac J Cancer Prev*, **14**, 3369-84.

Pope AC, Burnett TR, Thun JM (2002). Lung cancer, cardiopulmonary mortality, and long-term exposure to fine particulate air pollution. *J Am Med Assoc*, **287**, 1132-41.

Thumanu K, Pongpiachan S, Ho KF, Lee SC (2009). Characterization of organic functional groups, water-soluble ionic species and carbonaceous compound in PM_{10} from various emission sources in Songkhla Province, Thailand. Air Pollution XVII, WIT press, pp. 295-306.

US EPA (1991). Risk assessment guidance for superfund, volume I: human health evaluation manual, supplemental guidance: "Standard default exposure factors" interim final. OSWER Directive 9285.6-03, Washington D.C. March 25, 1991.

US EPA (1994). Methods for derivation of inhalation dosimetry. Washington DC: Office of Research and Development, Office of Health and Environmental Assessment. EPA/600/Z-92/001.

Whitby KT, Sverdrup GM (1980). California aerosols: their physical and chemical characteristics, in The Character and Origins of Atmospheric Aerosols. Advance in Environ. Sci. Technol, 9, Wiley, New York, NY.

Zielinska B, Sagebiel J, Arnott PW (2004). Phase and size distribution of polycyclic aromatic hydrocarbons in diesel and gasoline vehicle emissions. *Environ Sci Technol*, **38**, 2557-67.